

# Vestigial Order from an Excitonic Mother State in Kagome Superconductors $AV_3Sb_5$

Julian Ingham,<sup>1</sup> Ronny Thomale,<sup>2</sup> and Harley D. Scammell<sup>3,\*</sup>

<sup>1</sup>*Department of Physics, Columbia University, New York, NY, 10027, USA*

<sup>2</sup>*Institute for Theoretical Physics and Astrophysics,  
University of Würzburg, D-97074 Würzburg, Germany*

<sup>3</sup>*School of Mathematical and Physical Sciences, University of Technology Sydney, Ultimo, NSW 2007, Australia*  
(Dated: March 6, 2025)

Alongside high-temperature charge order and superconductivity, kagome metals exhibit signatures of time-reversal symmetry breaking and nematicity which appear to depend strongly on external perturbations such as strain and magnetic fields, posing a fundamental challenge for conceptual reconciliation. We develop a theory of vestigial order descending from an excitonic mother state in  $AV_3Sb_5$  ( $A=K,Rb,Cs$ ), which develops around  $T_* \simeq 40$  K. The application of external fields stabilises a subset of the phase-melted order parameter manifold, referred to as a vestigial state, producing a symmetry-breaking response which depends on the applied probe. Our theory reproduces the observations of piezomagnetism, electric magnetic chiral anisotropy, absence of Kerr rotation, unusual elastoresistance response, and superconducting diode effect. Our proposed excitonic mother state accounts for probe-dependent symmetry breaking patterns without fine-tuning, and predicts additional signatures accessible through optical spectroscopy.

## I. INTRODUCTION

Kagome metals have emerged as a rich playground for the exploration of correlated phases of matter, and developed into one of the most vibrant fields in contemporary condensed matter physics due to the propensity of these systems to host exotic electronic orders [1–17]. The recently discovered superconducting family  $AV_3Sb_5$  ( $A=K,Rb,Cs$ ) has attracted immense attention due to its exotic principal phenomenology of high-temperature exotic charge order which sets in around  $T_{CDW} \simeq 100$  K, coexisting with unconventional superconductivity with  $T_c \simeq 2$  K [18–44]. As theoretical proposals continue to proliferate exciting predictions – such as orbital current phases, nematic orders, and pair density wave superconductivity [45–57] – the accumulating experimental phenomenology from multiple measurement techniques such as surface spectroscopy, transport, and thermodynamics has proven as intriguing as it is difficult to reconcile within a universal framework [58].

This particularly applies to the intermediate regime  $T_c < T < T_{CDW}$ , in which experiments have presented seemingly contradictory results. A recurring question has been whether the CDW appearing at  $T_{CDW}$  breaks rotational or time-reversal symmetry (TRS). Initial reports claimed signatures of TRS breaking at  $T_{CDW}$  – pointing to a large Hall conductivity [20], an increase in the relaxation rate in  $\mu$ SR [22, 23], magnetic field-tuned switching of the CDW Bragg peaks [23], and Kerr rotation [24]. Yet the experimental status has significantly complicated since these initial reports – no hysteresis is seen in the Hall conductivity [20, 21], many experiments see no switching of the Bragg peaks [25, 59] or Kerr rotation [26], and while  $\mu$ SR does see a feature near  $T_{CDW}$ , the largest increase in relaxation rate is observed near  $T_* \simeq 40$  K [60].

Recent experiments suggest a clarifying perspective on these unusual properties. When placed in an ultra low-strain environment,  $CsV_3Sb_5$  shows evidence of inversion symmetry breaking in nonlinear transport near  $T_*$ , known as electric-magnetic chiral anisotropy (eMChA), while these signatures rapidly vanish in small strain fields [61]. Magnetic torque measurements also observe thermodynamic evidence of a magnetic transition around  $T_*$  [62], at which a large and unusual elastoresistance response in the symmetric  $A_{1g}$  channel is observed [63]. Also near  $T_*$ , a giant piezomagnetic response appears [64], and small out-of-plane magnetic fields result in threefold rotational symmetry breaking [65]. Of particular note is the probe-dependence of the symmetry breaking –  $c$ -axis strain or out-of-plane magnetic fields eliminate eMChA [66], while low-strain samples *only* present signatures of rotational symmetry breaking in applied magnetic fields [65, 67]. Taken together, these experiments demonstrate that in the absence of perturbations,  $CsV_3Sb_5$  does not break TRS nor rotational symmetries in the absence of strain or magnetic fields, yet develops some kind of unusual electronic phase near  $T_*$  that exhibits a drastic symmetry breaking response to external probes. This large inherent sensitivity of the broken symmetries to external conditions rationalises the contradictory results from different experimental groups.

From a synoptic experimental perspective on kagome superconductors, this presents an exciting puzzle: is it possible to capture all such features through a single organisational principle? The outset might bear some similarities to the pseudogap phase in high-temperature copper oxide superconductors, where the system’s response likewise sensitively depends on the precise parameters and external conditions [68]. Cuprates witnessed the pseudogap phase as an intricate interpolation phenomenon between the dominant magnetic phase at half filling and the unconventional superconducting phase at sufficient doping; in this context the concept of intertwined orders has arisen,

\* harley.scammell@uts.edu.au

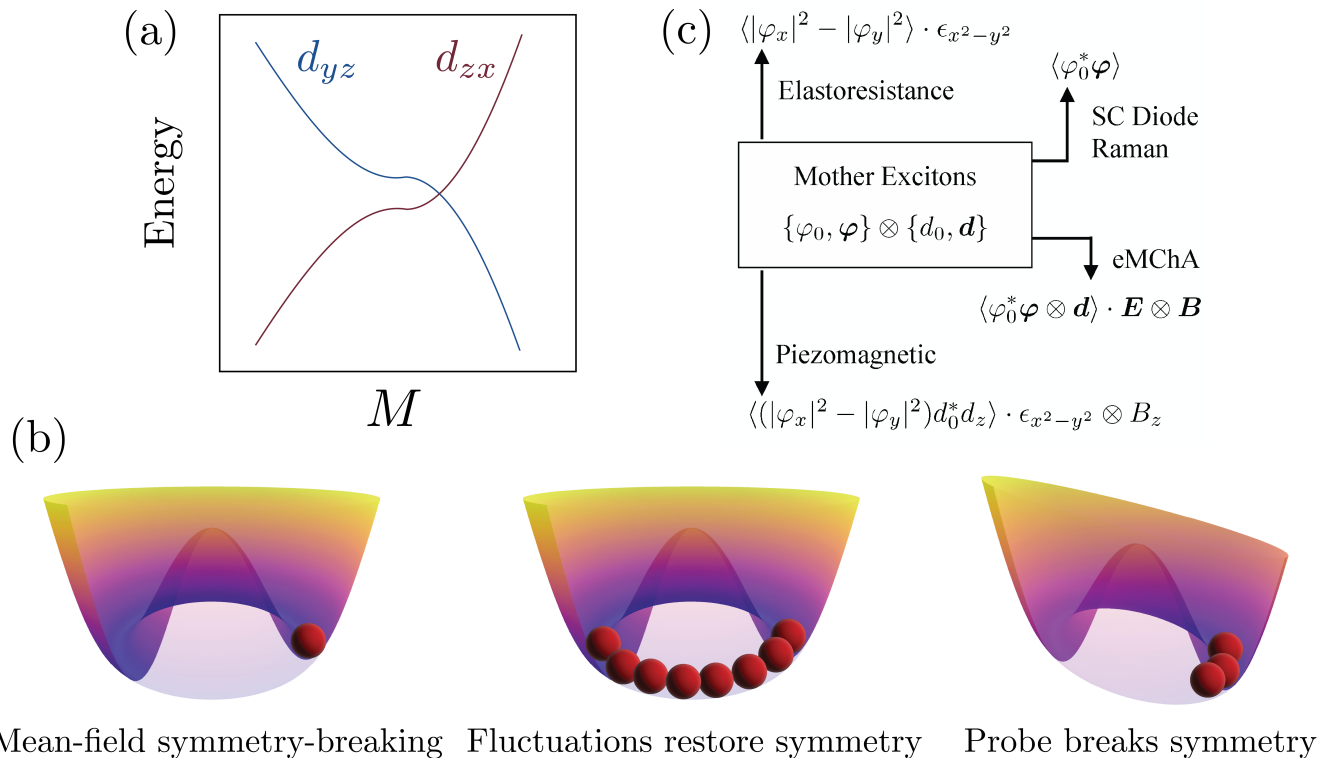


FIG. 1: **Probe-dependent symmetry breaking from an excitonic mother state.** (a) The bandstructure of  $AV_3Sb_5$  features twofold van Hove singularities near the  $M$  point with opposite concavity, originating from the  $d_{xz}$  and  $d_{yz}$  vanadium orbitals. These bands are prone towards an excitonic instability which hybridises the bands. (b) Concept of a vestigial mother state: an excitonic order parameter breaks a large set of symmetries at mean-field level, represented by the red ball in a minimum of the wine bottle potential, but fluctuations between different symmetry-related ground states restore the symmetry on average. Applying an external probe quenches these fluctuations, resulting in a large symmetry-breaking response, represented by a strong accumulation of spectral weight in a symmetry-breaking minimum of the free energy. (c) Different external probes – applied strain, electric and magnetic fields – stabilise different vestigial orders, resulting in a range of unconventional responses.

via which the comparable multiple ordering propensities of a correlated electronic system are more naturally explained than from merely competing orders [69]. Cuprates further suggest a pair density wave as potential “mother description”, out of which the charge orders derive as vestigial states [70]. By analogy, the key ordering pillars of kagome metals would be charge order and superconductivity. Those ordered domains are, however, much less well-understood than for the high- $T_c$  cuprates, and exhibit a totally unique set of symmetry-breaking patterns.

Existing theories have attempted to rationalize the experimental phenomenology of kagome metals through multiple CDW orders appearing simultaneously at  $T_*$  [56, 64, 71]. Such ansätze are somewhat contrived due to the implicit fine tuning in positing multiple coincident order parameters. Instead, we propose a different conceptual framework to unify these observations: that of a new phase of matter, a vestigial excitonic state. The bandstructure of kagome metals such as  $AV_3Sb_5$  features electron- and hole-like bands close to the Fermi level. From there, it has been proposed that  $d$ -wave excitonic order is a

natural ground state for repulsive interactions, and can coexist with CDW order [8]. In a quasi-two-dimensional system, such a state could serve as a “mother state” that is melted by phase fluctuations. We show that external probes such as field or strain stabilise bilinears of this melted order parameter, i.e. form vestigial orders [72–75]. The symmetry of the vestigial order depends on the applied probe (Fig. 1b); here we show that the richness of the spin and orbital structure of this melted order parameter manifold naturally synthesises a large range of experimental observations, presenting a unified theory for kagome superconductors such as  $CsV_3Sb_5$ . Building on this synthesis, we predict signatures of our putative mother state in optical spectroscopy and STM.

By comparison to the pair density wave as a tentative parent state of high- $T_c$  cuprates, our proposal can be interpreted as a description for kagome metals hinging on excitonic fluctuations inherited from a melted excitonic mother state.

## II. RESULTS

### A. Parent excitonic order

We begin with a discussion of the orbital content of the bands in  $AV_3Sb_5$ . ARPES observes two oppositely dispersing bands near the Fermi level, which arise from the multiplet of vanadium  $d$ -orbitals [76, 77]; as illustrated schematically in Fig. 1a. The minimal two-band model we employ comprises  $d_{zx}, d_{yz}$  orbitals – for more discussion of the bandstructure and orbital content see the Supplementary Material (SM). Describing the vHS nearest to the Fermi level (Fig. 1), the single particle Hamiltonian is given by

$$H_0 = \sum_{\mathbf{k}} c_{\mathbf{k}}^\dagger (\varepsilon_{\mathbf{k}}^c - \mu) c_{\mathbf{k}} + v_{\mathbf{k}}^\dagger (\varepsilon_{\mathbf{k}}^v - \mu) v_{\mathbf{k}} \quad (2.1)$$

where  $c_{\mathbf{k}}^\dagger, (v_{\mathbf{k}}^\dagger)$  are creation operators for conduction (valence) electrons, with spin indices suppressed. The U(1) symmetry manifests as independent global U(1) phases of the  $c_{\mathbf{k}}^\dagger, v_{\mathbf{k}}^\dagger$  electrons; in the limit where this symmetry is exact, the conduction and valence bands correspond to pure  $d_{zx}$  and  $d_{yz}$  content. The chemical potential is tuned to the approximate vicinity of the  $M$ -points, near which there is an approximate spectral particle-hole symmetry  $\varepsilon_{M_i+\mathbf{k}}^v \simeq -\varepsilon_{M_i+\mathbf{k}}^c$ . Finally, we make special note that, at the  $M$ -points,  $c_{\mathbf{k}}^\dagger (v_{\mathbf{k}}^\dagger)$  create  $p$ -type ( $m$ -type) vHS states [5]; these are inversion even (odd).

The opposite dispersion of these two bands results in an instability towards an excitonic condensate, as theoretically conjectured in Ref. [8], where a tendency towards  $d$ -wave excitonic pairing – i.e. particle-hole pairing in a two-dimensional (2D) irreducible symmetry representation (irrep) – is found. We take this premise as a starting point for the present work, and elevate it to form a basis for our theory of a vestigial mother state of kagome metals.

Utilizing the results of Ref. [8], we specialize to pairing in a 2D irrep. The pairing term in the Hamiltonian takes the form

$$H_{\text{pair}} = \sum_{\mathbf{k}} M_{\mathbf{k}} c_{\mathbf{k}}^\dagger v_{\mathbf{k}} + \text{h.c.}, \quad M_{\mathbf{k}} = (\boldsymbol{\varphi} \cdot \boldsymbol{\mathcal{E}}_{\mathbf{k}}) d_{\mu} s_{\mu} \quad (2.2)$$

where  $s_{\mu}$  ( $\mu = 0, x, y, z$ ) are Pauli matrices acting on spin and  $\boldsymbol{\mathcal{E}}_{\mathbf{k}}$  is a two-component basis function that represents the different possible 2D irreps. Combining states from vHS of opposite parity,  $p$ -type/ $m$ -type, and with a  $d$ -wave pairing, as per [8], produces an order parameter which transforms overall as the  $E_{1u}$  irrep [78], which we parametrize as

$$\boldsymbol{\mathcal{E}}_{\mathbf{k}}^{E_{1u}} = (X_{\mathbf{k}}, Y_{\mathbf{k}}) \in E_{1u}$$

where  $X_{\mathbf{k}}, Y_{\mathbf{k}}$  transform as  $k_x, k_y$ . The order parameter in Eq. (2.2) is composed of two complex vectors

$$\boldsymbol{\varphi} = (\varphi_x, \varphi_y), \quad \bar{\mathbf{d}} = (d_0, d_x, d_y, d_z). \quad (2.3)$$

The basis function  $\boldsymbol{\varphi} \in E_{1u}$  transforms as a vector under spatial rotations. The three-vector  $\mathbf{d} = (d_x, d_y, d_z)$  transforms as an SO(3) pseudo-vector under spin-rotations and corresponds physically to spin-triplet pairing, while  $d_0$  is a scalar and corresponds to spin-singlet pairing. We will denote the order parameter as the tensor product of the spatial and spin components  $\Delta = \boldsymbol{\varphi} \otimes \bar{\mathbf{d}}$ .

In the absence of exchange interactions, there is separate conservation of the spin for each flavour, i.e. spin SU(2)×SU(2) symmetry – which manifests as an SO(4) spin symmetry of the excitonic order parameters, implying that spin-singlet and triplet states form a degenerate manifold. Including exchange terms, the order parameter decomposes into singlet and triplet channels. Our conclusions do not rely on strict SO(4) symmetry; in the SM we allow for perturbations away from this limit.

Finally, previous *ab initio* studies show explicit breaking of orbital U(1) symmetry [45]. To account for this, we additionally introduce a U(1)-breaking background field term  $\varphi_0 \chi_{\mathbf{k}}^{B_{2u}} c_{\mathbf{k}}^\dagger v_{\mathbf{k}}$  into the pairing Hamiltonian (2.2), where  $\varphi_0$  is a spin-independent complex number with phase set by the microscopic details of the orbitals, while  $\chi_{\mathbf{k}}^{B_{2u}}$  is a basis function in the  $B_{2u}$  irrep. Crucially, this background field breaks the global U(1) but does not break crystalline point group  $D_{6h}$ , i.e. transforms as the  $A_{1g}$  irrep. The background field  $\varphi_0$  allows for the  $\Phi_{E_{1u}}$  vestigial of Table I.

### B. Vestigial order

The excitonic state breaks a set of continuous approximate symmetries – the SO(4) arising from near degeneracy of singlet and triplet order, along with the approximate U(1) particle-hole number symmetry, and so in two dimensions this order parameter should in fact melt due to fluctuations,  $\langle \Delta \rangle \simeq 0$ . The importance of fluctuations to the physics of  $T_*$  is underscored by the apparent broadness of the transition, seen for in e.g. piezomagnetism [65]. On the other hand, vestigial orders – products of different components of the order parameter manifold we

Spatial		Spin	
Label	Content	Label	Content
$\Phi_{A_{1g}}$	$\boldsymbol{\varphi}^* \cdot \boldsymbol{\varphi}$	$D_{\text{scalar}}$	$\bar{\mathbf{d}}^* \cdot \bar{\mathbf{d}}$
$\Phi_{A_{2g}}$	$i\boldsymbol{\varphi}^* \times \boldsymbol{\varphi}$	$D_{\text{axial}}$	$d_0^* \mathbf{d}$
$\Phi_{E_{2g}}$	$\begin{pmatrix} \varphi_x^* \varphi_x - \varphi_y^* \varphi_y \\ \varphi_x^* \varphi_y + \varphi_y^* \varphi_x \end{pmatrix}$	$\tilde{D}_{\text{axial}}$	$\mathbf{d}^* \times \mathbf{d}$
$\Phi_{E_{1u}}$	$\varphi_0^* \boldsymbol{\varphi}$	-	-

TABLE I: Possible vestigial orders decomposed into spatial and spin contributions  $\Phi_{\Gamma} \otimes D_{\Gamma_s}$ .

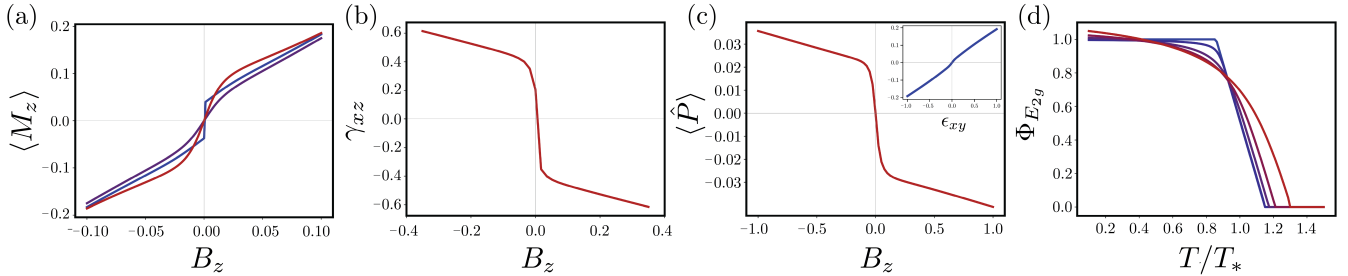


FIG. 2: **Unconventional responses of the excitonic mother state.** (a) AHE with increasing values of strain from blue to red, as measured by the magnetization  $\langle M_z \rangle$ . (b) The eMChA response, defined so that the resistance receives a contribution  $\gamma_{ij} B_i I_j$ . (c) Piezomagnetic response, measured by the expectation value of  $\hat{P} = \Phi_{E_{2g}} \otimes D''_{\text{axial}}$ , which requires both non zero field and strain. Red shows the dependence of  $\hat{P}$  on field for fixed strain, and blue the dependence on strain for fixed  $B_z \neq 0$ . (d) Transport anisotropy measured by the magnitude of the order parameter  $\Phi_{E_{2g}}$ , for incrementally increasing  $B_z$ . The free energy and explicit values of the parameters employed are presented in the SM.

denote by  $V[\Delta^*, \Delta]$  – can be invariant under the continuous symmetries, breaking only discrete ones [73]. These states are stable against fluctuation effects.

We neglect spin-orbit coupling, and thereby treat spin and spatial contributions separately, denoting the symmetries of the vestigial orders as a product of a spatial part  $\Phi_\Gamma$ , a bilinear in  $\varphi$ , and spin part  $D_{\Gamma_s}$ , a bilinear in  $\vec{d}$ , via  $V[\Delta^*, \Delta] = \Phi_\Gamma \otimes D_{\Gamma_s}$ . In each case the irreps are labelled by  $\Gamma = \{A_{1g}, A_{2g}, E_{2g}, E_{1u}\}$  and  $\Gamma_s = \{\text{scalar}, \text{axial-vector}\}$ . Table I lists the structure of the spatial and spin vestigials; their connection to applied probes is shown in Fig. 1b.

Our theoretical scenario is illustrated in Fig. 1b: with the application of strain or fields, a particular vestigial combination is induced out of the melted order parameter manifold, producing a ground state expectation value which depends on the nature of the external probe. To determine the precise response to external perturbations, we write down the coupling of the excitonic order parameter with strain and electromagnetic fields via the Landau-Ginzburg approach,

$$\mathcal{F} = \mathcal{F}_0[\Delta] + \delta\mathcal{F}[\Delta; \mathbf{E}, \mathbf{B}, \epsilon] \quad (2.4)$$

where  $\mathcal{F}_0[\Delta]$  is a function of the excitonic order parameter, while  $\delta\mathcal{F}[\Delta; \mathbf{E}, \mathbf{B}, \epsilon]$  contains the allowed couplings to strain  $\epsilon$  and electric/magnetic fields; we present the full expressions in the SM. Via minimisation of the free energy subject to various combinations of external fields, our task is to confirm: (1) the existence of vestigial order  $\langle V[\Delta^*, \Delta] \rangle \neq 0$ , and (2) that these vestigials are able to explain the array of observed responses near  $T_*$ .

### C. Unconventional responses

#### 1. Large induced Hall effect and absence of Kerr rotation

At zero magnetic field no anomalous Hall effect (AHE) is observed experimentally, however a large Hall conductance is induced by an applied field, which is observed to be nonlinear in  $B$  [20].

In the absence of strain, the ground state of  $\mathcal{F}_0$ , generically favours chiral spatial order  $\Phi_{A_{2g}} = i\varphi^* \times \varphi$ , since this nodeless order parameter maximises the condensate energy. This bilinear transforms as an out-of-plane Ising magnetisation, and breaks TRS and mirror symmetries. Yet, in the presence of strain, the favoured bilinear is a rotational symmetry breaking nematic state  $\Phi_{E_{2g}} = |\varphi_x|^2 - |\varphi_y|^2$ . Moreover, in the presence of strain and  $B_z$ , our theory predicts a piezomagnetic response (see Sec. II C 3), which generates a magnetization that is non-linear in  $B_z$ , as shown in Fig. 2a. Hence, our framework explains the results of Ref. [20] by suggesting that their samples contained an intrinsic or extrinsic strain field, a common occurrence in kagome metals.

The lack of zero-field AHE implies the lack of Kerr rotation, consistent with experiment [26]. Conversely, our arguments suggest that ultra low strain samples should in fact exhibit zero field AHE and Kerr rotation.

#### 2. eMChA

Refs. [61, 66] observe an anisotropic magnetoelectric contribution to the resistance,  $R(\mathbf{B}, \mathbf{I}) = R_0(1 + \mu^2 B^2 + \gamma_{ij} B_i I_j)$ . The term  $\mu^2 B^2$ , where  $\mu$  is the carrier mobility, is the ordinary magnetoresistance of non-magnetic metals, whereas the term proportional to the tensor  $\gamma_{ij}$  can only be nonzero when inversion symmetry is broken. The experimental setup takes  $\mathbf{B} = B\hat{x}$  and  $\mathbf{I} = I\hat{z}$ , and finds that a small out-of-plane  $B_z$  changes the sign of  $\gamma_{ij}$ . We find that these external perturbations couple to the exciton vestigial  $\gamma_{ij} \propto \text{Re}[(\Phi_{E_{1u}})_j \otimes (D_{\text{axial}})_i]$ , triggering a transition out of the  $A_{2g}$  state. Computing the eMChA tensor from the free energy (2.4), we find a nonzero response with  $B_z$  (Fig. 2b).

#### 3. Piezomagnetism

STM [64] and transport [65] report a piezomagnetic response tensor,  $P_{ijk}$ , such that  $\epsilon_{xy} = P_{xy} B_z \in E_{2g}$ ,

i.e. produces a strain that changes sign with  $B_z$ . In our theory, strain induces  $\hat{P} \propto \Phi_{E_{2g}} \otimes D''_{\text{axial}}$ ; our computed piezomagnetic response changes sign with  $B_z$ , Fig. 2d. Physically, the nematic vestigial can be favoured either via small extrinsic strains of the lattice or via coupling to a  $C_3$ -breaking CDW.

#### 4. Electrostriction

Ref. [64] also measures an electro-striction response, i.e. an electric field induced by applied strain. The electro-striction response tensor is  $\chi_{ijkl}$ , whereby  $\varepsilon_{xy} = \chi_{xyxy} E_x E_y \in E_{2g}$ . Already  $\varepsilon_{xy} E_x E_y \in A_{1g} + E_{2g}$  and hence is allowed simply by the crystal symmetries without recourse to an order parameter. However, we note that the  $E_{2g}$  part of  $\varepsilon_{xy} E_x E_y$  can couple to the  $E_{2g}$  vestigial, and hence the onset of vestigial order is expected to enhance this response.

#### 5. Elastoresistance

Experiments [63, 79] report a highly unusual elastoresistance response: upon applying strain, one measures  $\Delta R_{A_{1g}} = R_{xx} + R_{yy}$  and  $\Delta R_{E_{2g}} = R_{xx} - R_{yy}$ , and finds a large response in the  $A_{1g}$  channel with negligible contribution in the  $E_{2g}$  channel – which naively seems to be at odds with the observation of large strain-induced transport anisotropy [65], yet the peak in  $A_{1g}$  is further evidence of a phase transition occurring at  $T_*$ . While Ref. [63] claims an  $E_{2g}$  response is absent, there is clearly a feature at  $T_*$ , especially in the transverse technique [80].

Interestingly, the vestigial  $E_{2g} = (E_{1u})^2$  transforms with an effective angular momentum of  $\ell = 10$  (see the SM), while strain couples at leading order with  $\ell = 2$ . This results in a suppression of the coupling between the  $E_{2g}$  and strain in elastoresistance. To demonstrate this, first note the underlying exciton takes the functional form

$$\varphi \cdot \mathcal{E}_{\mathbf{k}} = (X_{\mathbf{k}}^2 - Y_{\mathbf{k}}^2) Y_{\mathbf{k}} (3X_{\mathbf{k}}^2 - Y_{\mathbf{k}}^2) \quad (2.5)$$

The bilinear

$$\Phi_{\mathbf{k}} \sim (\varphi \cdot \mathcal{E}_{\mathbf{k}})^2 = \Phi_{\mathbf{k}}^{A_{1g}} + \Phi_{\mathbf{k}}^{E_{2g}}, \quad (2.6)$$

is a mixture of  $A_{1g}$  and  $E_{2g}$  in the  $\ell = 10$  harmonic. At leading order strain transforms as  $\epsilon_{\mathbf{k}}^{A_{1g}} \sim X_{\mathbf{k}}^2 + Y_{\mathbf{k}}^2$ ,  $\epsilon_{\mathbf{k}}^{E_{2g}} \sim X_{\mathbf{k}}^2 - Y_{\mathbf{k}}^2$ ; and using that resistive anisotropy is linearly proportional electronic anisotropy (see e.g. Ref. [81]) we compute the overlap

$$\Delta R_{A_{1g}} \sim \sum_{\mathbf{k}} \Phi_{\mathbf{k}} \epsilon_{\mathbf{k}}^{A_{1g}}, \quad \Delta R_{E_{2g}} \sim \sum_{\mathbf{k}} \Phi_{\mathbf{k}} \epsilon_{\mathbf{k}}^{E_{2g}}. \quad (2.7)$$

We find that  $\Delta R_{A_{1g}} / \Delta R_{E_{2g}} \simeq 15$ . We suggest that this relative suppression of  $\Delta R_{E_{2g}}$  explains the large peak in the  $A_{1g}$  susceptibility alongside a small ratio of the  $E_{2g}$  and  $A_{1g}$  responses.

#### 6. Superconducting diode effect

Recently a zero-field superconducting diode effect has been observed [82]. Such an effect requires broken TRS,  $I$  and  $C_{2z}$  [83, 84]; crucially, inversion symmetry must be broken in the normal state for this effect to arise. The excitonic vestigial  $\Phi_{E_{1u}}$  is sufficient to break  $I$  and  $C_{2z}$ , satisfying the symmetry requirements for a superconducting diode effect.

#### 7. Raman spectroscopy

Below  $T_*$ , Raman spectroscopy should observe new  $A_{1g}, E_{2g}$  modes directly, as well as the appearance of a peak due to the  $E_{1u}$  phonon which is Raman inactive above  $T_*$ , but becomes visible due to the coupling with  $E_{1u}$  excitons.

The Raman probe  $J_{XX}$  couples the  $E_{1u}$  phonon doublet  $\mathbf{O}_{E_{1u}} = (O_X, O_Y)$  to the  $E_{1u}$  order via  $J_{XX} \mathbf{O}_{E_{1u}} \cdot \Phi_{E_{1u}}$ . Defining axes such condensation occurs with  $\Phi_X > 0$  and  $\Phi_Y = 0$ , implies that the phonon doublet  $(O_X, O_Y)$  is split, with  $O_X$  now possessing lower excitation energy due to coupling with  $\Phi_X$ . Rotating the polarisation of incident light,  $J_{RR}^\phi = \cos^2 \phi J_{XX} + \sin^2 \phi J_{YY}$ ; we therefore expect a dominant contribution

$$J_{RR}^\phi \mathbf{O}_{E_1} \cdot \Phi_{E_1} = \cos^2 \phi J_{XX} O_X \Phi_X. \quad (2.8)$$

Hence, *one should observe a Raman peak with a twofold rotational dependence in  $\phi$* . Recent studies [85] and unpublished data [86] have observed such a mode with two-fold dependence that sharpens near  $T_*$  [87].

### III. DISCUSSION

#### A. Subsidiary CDW orders

A final interesting effect we discuss is the induction of subsidiary CDW orders via the excitonic vestigial state. We have claimed that in zero external fields the dominant vestigial is  $\Phi_{E_{1u}} D_{\text{scalar}}$ ; we set  $D_{\text{scalar}} = 1$  for clarity below. Denoting a charge density wave order with wavevector  $\mathbf{M}_i$  transforming with symmetry irrep  $\Gamma$  (w.r.t. little group  $C_{2h}$  at the  $\mathbf{M}$  point) as  $\mathcal{C}_{\mathbf{M}_i}^\Gamma$ , the allowed couplings to CDW orders are

$$\mathcal{F}_{\text{mix}} = \left[ \alpha_1 \left( \mathcal{C}_{\mathbf{M}_i}^{A_g} \mathbf{V}_{ij} \mathcal{C}_{\mathbf{M}_j}^{A_u} \right) + \alpha_2 \left( \mathcal{C}_{\mathbf{M}_i}^{A_g} \mathbf{V}_{ij} \mathcal{C}_{\mathbf{M}_j}^{B_u} \right) \right] \cdot \Phi_{E_{1u}}$$

where  $\mathbf{V}_{ij}$  is a doublet of  $3 \times 3$  matrices  $V^{(1)} = \text{diag}(1, -2, 1)$  and  $V^{(2)} = \text{diag}(1, 0, -1)$ . Here we have labeled the CDWs via the little group at  $M$ -points,  $C_{2h}$ . It follows that  $B_u, A_u$  CDW orders become admixed via the  $E_{1u}$  exciton vestigial [88] – the resulting phase diagram is sketched in Fig. 3. One concrete prediction of this scenario is the hierarchy of order parameter magnitudes illustrated by the vertical axis.

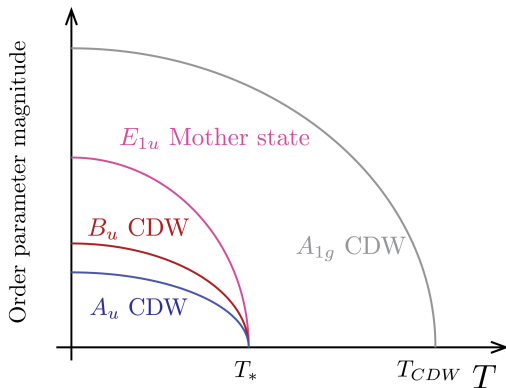


FIG. 3: **Induced CDW orders.** The proposed symmetry breaking pattern:  $A_g$  CDW at appears at  $T_{CDW}$  followed by vestigial mother state at  $T_*$ , here taken to be  $\Phi_{E_{1u}}$ , which necessarily admixes  $A_u, B_u$  CDWs.

## B. Conclusions and outlook

Our work produces a unified organizational principle to reconcile the diverse and seemingly contradictory experimental responses observed in kagome metals. At its core is a fluctuation-melted excitonic mother state, whose vestigial orders hosts a range of possible symmetry-breaking patterns, which emerge or are enhanced under the application of external fields.

To demonstrate the utility of this framework, we employed explicit modeling via a Landau free energy treatment to account for the complex phenomenology observed across various experiments on kagome metal  $\text{CsV}_3\text{Sb}_5$ . Taken together, our findings provide strong evidence that vestigial orders explain the puzzling observations near  $T_*$ , challenging the prevailing view that CDW order alone

underlies the rich phenomenology observed below  $T_{CDW}$ , including  $T_*$ .

Prospectively, we suggest experiments aimed at directly probing the proposed excitonic mother state:

- (i) Optical spectroscopy: The evolution of excitonic bound-state spectra in the range  $T_* < T < T_{CDW}$  could provide evidence for or against the formation of the excitonic mother state. If the excitation energy vanishes as  $T_*$  is approached, this would be consistent with an excitonic mother state.
- (ii) Scanning tunneling microscopy (STM): Since STM is sensitive to spatial symmetries, a detailed analysis near  $T_*$  would be particularly informative – in particular a comparison of the magnitude of  $E_{1u}$  and CDW  $A_u/B_u$  order parameter magnitudes, c.f. Fig. 3.
- (iii) Symmetry-selective ultrasound experiments: By measuring the system’s elastic moduli, these experiments can effectively uncover the point-group symmetries of order parameters [89, 90].

The possible destruction of the excitonic mother state with pressure or doping may account for abrupt changes in the superconducting and magnetic properties observed in  $\text{AV}_3\text{Sb}_5$ ; exploring the influence of such perturbations on the responses discussed above will yield important insights into the nature of this unconventional mother state.

## ACKNOWLEDGEMENTS

We thank Riccardo Comin, Chenhao Jin, and Dongjin Oh for helpful discussions and comments. J.I. is supported by NSF Career Award No. DMR-2340394.

- 
- [1] E. Tang, J.-W. Mei, and X.-G. Wen, “High-temperature fractional quantum Hall states,” *Phys. Rev. Lett.* **106**, 236802 (2011).
  - [2] D. Green, L. Santos, and C. Chamon, “Isolated flat bands and spin-1 conical bands in two-dimensional lattices,” *Phys. Rev. B* **82**, 075104 (2010).
  - [3] S.-L. Yu and J.-X. Li, “Chiral superconducting phase and chiral spin-density-wave phase in a Hubbard model on the kagome lattice,” *Phys. Rev. B* **85**, 144402 (2012).
  - [4] M. L. Kiesel, C. Platt, and R. Thomale, “Unconventional fermi surface instabilities in the kagome Hubbard model,” *Phys. Rev. Lett.* **110**, 126405 (2013).
  - [5] M. L. Kiesel and R. Thomale, “Sublattice interference in the kagome Hubbard model,” *Phys. Rev. B* **86**, 121105 (2012).
  - [6] T. Li, M. Geier, J. Ingham, and H. D. Scammell, “Higher-order topological superconductivity from repulsive interactions in kagome and honeycomb systems,” *2D Materials* **9**, 015031 (2021).
  - [7] A. Wenger, A. Consiglio, H. Hohmann, M. Dürnagel, F. O. von Rohr, H. D. Scammell, J. Ingham, D. Di Sante, and R. Thomale, “Theory of unconventional magnetism in a cu-based kagome metal,” *arXiv preprint arXiv:2411.03563* (2024).
  - [8] H. D. Scammell, J. Ingham, T. Li, and O. P. Sushkov, “Chiral excitonic order from twofold van hove singularities in kagome metals,” *Nature Communications* **14**, 605 (2023).
  - [9] J. Ingham, A. Consiglio, D. di Sante, R. Thomale, and H. D. Scammell, “Theory of excitonic order in  $\text{scv}_6\text{sn}_6$ ,” *arXiv preprint arXiv:2410.16365* (2024).
  - [10] J.-W. Dong, Z. Wang, and S. Zhou, “Loop-current charge density wave driven by long-range Coulomb repulsion on the kagome lattice,” *Phys. Rev. B* **107**, 045127 (2023).
  - [11] J. B. Profe, L. Klebl, F. Grandi, H. Hohmann, M. Dürnagel, T. Schwemmer, R. Thomale, and D. M. Kennes, “Kagome Hubbard model from a functional renormalization group perspective,” *Physical Review Research* **6**, 043078 (2024).

- [12] P. K. Nag, R. Batabyal, J. Ingham, N. Morali, H. Tan, J. Koo, A. Consiglio, E. Liu, N. Avraham, R. Queiroz, *et al.*, “Pomeranchuk instability induced by an emergent higher-order van Hove singularity on the distorted kagome surface of  $\text{Co}_3\text{Sn}_2\text{S}_2$ ,” *arXiv preprint arXiv:2410.01994* (2024).
- [13] F. Z. Yang, X. Huang, H. Tan, A. Kundu, S. Kim, M. Thinel, J. Ingham, A. Rajapitamahuni, C. Nelson, Y. Q. Cai, E. Vescovo, W. R. Meier, D. Mandrus, B. R. Ortiz, A. N. Pasupathy, B. Yan, and H. Miao, “Formation of frustrated charge density waves in kagome metal  $\text{Lu}_6\text{Sn}_6$ ,” *arXiv preprint arXiv:2502.20593* (2025).
- [14] Y.-X. Jiang, S. Shao, W. Xia, M. M. Denner, J. Ingham, M. S. Hossain, Q. Qiu, X. Zheng, H. Chen, Z.-J. Cheng, *et al.*, “Van Hove annihilation and nematic instability on a kagome lattice,” *Nat. Mater.* **23**, 1214 (2024).
- [15] Y. Wang, H. Wu, G. T. McCandless, J. Y. Chan, and M. N. Ali, “Quantum states and intertwining phases in kagome materials,” *Nature Reviews Physics* **5**, 635 (2023).
- [16] J.-X. Yin, B. Lian, and M. Z. Hasan, “Topological kagome magnets and superconductors,” *Nature* **612**, 647 (2022).
- [17] T. Neupert, M. M. Denner, J.-X. Yin, R. Thomale, and M. Z. Hasan, “Charge order and superconductivity in kagome materials,” *Nat. Phys.* **18**, 137 (2022).
- [18] B. R. Ortiz, L. C. Gomes, J. R. Morey, M. Winiarski, M. Bordelon, J. S. Mangum, I. W. H. Oswald, J. A. Rodriguez-Rivera, J. R. Neilson, S. D. Wilson, E. Ertekin, T. M. McQueen, and E. S. Toberer, “New kagome prototype materials: discovery of  $\text{KV}_3\text{Sb}_5$ ,  $\text{RbV}_3\text{Sb}_5$ , and  $\text{CsV}_3\text{Sb}_5$ ,” *Phys. Rev. Mater.* **3**, 094407 (2019).
- [19] B. R. Ortiz, S. M. L. Teicher, Y. Hu, J. L. Zuo, P. M. Sarte, E. C. Schueller, A. M. M. Abeykoon, M. J. Krogstad, S. Rosenkranz, R. Osborn, R. Seshadri, L. Balents, J. He, and S. D. Wilson, “ $\text{CsV}_3\text{Sb}_5$ : A  $\mathbb{Z}_2$  topological kagome metal with a superconducting ground state,” *Phys. Rev. Lett.* **125**, 247002 (2020).
- [20] S.-Y. Yang *et al.*, “Giant, unconventional anomalous Hall effect in the metallic frustrated magnet candidate,  $\text{KV}_3\text{Sb}_5$ ,” *Science Advances* **6**, eabb6003 (2020).
- [21] D. Chen *et al.*, “Anomalous thermoelectric effects and quantum oscillations in the kagome metal  $\text{CsV}_3\text{Sb}_5$ ,” *Phys. Rev. B* **105**, L201109 (2022).
- [22] C. Mielke *et al.*, “Time-reversal symmetry-breaking charge order in a kagome superconductor,” *Nature* **602**, 245–250 (2022).
- [23] Y.-X. Jiang, J.-X. Yin, M. M. Denner, N. Shumiya, B. R. Ortiz, G. Xu, Z. Guguchia, J. He, M. S. Hossain, X. Liu, J. Ruff, L. Kautzsch, S. S. Zhang, G. Chang, I. Belopolski, Q. Zhang, T. A. Cochran, D. Multer, M. Litskevich, Z.-J. Cheng, X. P. Yang, Z. Wang, R. Thomale, T. Neupert, S. D. Wilson, and M. Z. Hasan, “Unconventional chiral charge order in kagome superconductor  $\text{KV}_3\text{Sb}_5$ ,” *Nat. Mater.* **20**, 1353 (2021).
- [24] Y. Xu, Z. Ni, Y. Liu, B. R. Ortiz, Q. Deng, S. D. Wilson, B. Yan, L. Balents, and L. Wu, “Three-state nematicity and magneto-optical Kerr effect in the charge density waves in kagome superconductors,” *Nat. Phys.* **18**, 1470 (2022).
- [25] H. Li *et al.*, “Rotation symmetry breaking in the normal state of a kagome superconductor  $\text{KV}_3\text{Sb}_5$ ,” *Nat. Phys.* **18**, 265 (2022).
- [26] D. R. Saykin *et al.*, “High resolution polar Kerr effect studies of  $\text{CsV}_3\text{Sb}_5$ : Tests for time-reversal symmetry breaking below the charge-order transition,” *Phys. Rev. Lett.* **131**, 016901 (2023).
- [27] H. Zhao, H. Li, B. R. Ortiz, S. M. Teicher, T. Park, M. Ye, Z. Wang, L. Balents, S. D. Wilson, and I. Zeljkovic, “Cascade of correlated electron states in the kagome superconductor  $\text{CsV}_3\text{Sb}_5$ ,” *Nature* **599**, 216 (2021).
- [28] H.-S. Xu *et al.*, “Multiband superconductivity with sign-preserving order parameter in kagome superconductor  $\text{CsV}_3\text{Sb}_5$ ,” *Phys. Rev. Lett.* **127**, 187004 (2021).
- [29] R. Gupta *et al.*, “Microscopic evidence for anisotropic multigap superconductivity in the  $\text{CsV}_3\text{Sb}_5$  kagome superconductor,” *npj Quantum Materials* **7**, 1 (2022).
- [30] W. Duan *et al.*, “Nodeless superconductivity in the kagome metal  $\text{CsV}_3\text{Sb}_5$ ,” *Science China Physics, Mechanics & Astronomy* **64**, 1 (2021).
- [31] H. Li, T. Zhang, T. Yilmaz, Y. Pai, C. Marvinney, A. Said, Q. Yin, C. Gong, Z. Tu, E. Vescovo, *et al.*, “Observation of unconventional charge density wave without acoustic phonon anomaly in kagome superconductors  $\text{AV}_3\text{Sb}_5$  ( $A = \text{Rb}, \text{Cs}$ ),” *Physical Review X* **11**, 031050 (2021).
- [32] N. Shumiya *et al.*, “Intrinsic nature of chiral charge order in the kagome superconductor  $\text{RbV}_3\text{Sb}_5$ ,” *Phys. Rev. B* **104**, 035131 (2021).
- [33] H. Miao, H. X. Li, W. Meier, A. Huon, H. N. Lee, A. Said, H. Lei, B. Ortiz, S. Wilson, J. Yin, *et al.*, “Geometry of the charge density wave in the kagome metal  $\text{AV}_3\text{Sb}_5$ ,” *Phys. Rev. B* **104**, 195132 (2021).
- [34] S. Ni *et al.*, “Anisotropic superconducting properties of kagome metal  $\text{CsV}_3\text{Sb}_5$ ,” *Chinese Physics Letters* **38**, 057403 (2021).
- [35] C. C. Zhu *et al.*, “Double-dome superconductivity under pressure in the V-based kagome metals  $\text{AV}_3\text{Sb}_5$  ( $A = \text{Rb}$  and  $\text{K}$ ),” *Phys. Rev. B* **105**, 094507 (2022).
- [36] K. Y. Chen *et al.*, “Double superconducting dome and triple enhancement of  $T_c$  in the kagome superconductor  $\text{CsV}_3\text{Sb}_5$  under high pressure,” *Phys. Rev. Lett.* **126**, 247001 (2021).
- [37] F. Du, S. Luo, B. R. Ortiz, Y. Chen, W. Duan, D. Zhang, X. Lu, S. D. Wilson, Y. Song, and H. Yuan, “Pressure-induced double superconducting domes and charge instability in the kagome metal  $\text{KV}_3\text{Sb}_5$ ,” *Phys. Rev. B* **103**, L220504 (2021).
- [38] Z. Zhang, Z. Chen, Y. Zhou, Y. Yuan, S. Wang, J. Wang, H. Yang, C. An, L. Zhang, X. Zhu, *et al.*, “Pressure-induced reemergence of superconductivity in the topological kagome metal  $\text{CsV}_3\text{Sb}_5$ ,” *Phys. Rev. B* **103**, 224513 (2021).
- [39] Z. Liang *et al.*, “Three-dimensional charge density wave and surface-dependent vortex-core states in a kagome superconductor  $\text{CsV}_3\text{Sb}_5$ ,” *Physical Review X* **11**, 031026 (2021).
- [40] B. R. Ortiz, S. M. Teicher, L. Kautzsch, P. M. Sarte, N. Ratchiff, J. Harter, J. P. Ruff, R. Seshadri, and S. D. Wilson, “Fermi surface mapping and the nature of charge-density-wave order in the kagome superconductor  $\text{CsV}_3\text{Sb}_5$ ,” *Physical Review X* **11**, 041030 (2021).
- [41] Y. M. Oey, B. R. Ortiz, F. Kaboudvand, J. Frassinetti, E. Garcia, R. Cong, S. Sanna, V. F. Mitrović, R. Seshadri, and S. D. Wilson, “Fermi level tuning and double-dome superconductivity in the kagome metal  $\text{CsV}_3\text{Sb}_{5-x}\text{Sn}_x$ ,” *Physical Review Materials* **6**, L041801 (2022).
- [42] M. Kang, S. Fang, J. Yoo, B. R. Ortiz, Y. M. Oey, J. Choi, S. H. Ryu, J. Kim, C. Jozwiak, A. Bostwick, *et al.*, “Charge order landscape and competition with superconductivity in kagome metals,” *Nat. Mater.* **22**, 186 (2023).

- [43] Z. Huang, H. Chen, H. Tan, X. Han, Y. Ye, B. Hu, Z. Zhao, C. Shen, H. Yang, B. Yan, *et al.*, “Revealing the orbital origins of exotic electronic states with Ti substitution in kagome superconductor  $\text{CsV}_3\text{Sb}_5$ ,” *Phys. Rev. Lett.* **134**, 056001 (2025).
- [44] M. S. Hossain, Q. Zhang, J. Ingham, J. Liu, S. Shao, Y. Li, Y. Wang, B. K. Pokharel, Z.-J. Cheng, Y.-X. Jiang, *et al.*, “Field induced density wave in a kagome superconductor,” *arXiv preprint arXiv:2501.13260* (2025).
- [45] X. Wu, T. Schwemmer, T. Müller, A. Consiglio, G. Savigiovanni, D. Di Sante, Y. Iqbal, W. Hanke, A. P. Schnyder, M. M. Denner, M. H. Fischer, T. Neupert, and R. Thomale, “Nature of unconventional pairing in the kagome superconductors  $\text{AV}_3\text{Sb}_5$  ( $A=\text{K}, \text{Kb}, \text{Cs}$ ),” *Phys. Rev. Lett.* **127**, 177001 (2021).
- [46] M. M. Denner, R. Thomale, and T. Neupert, “Analysis of charge order in the kagome metal  $\text{AV}_3\text{Sb}_5$  ( $A=\text{K}, \text{Rb}, \text{Cs}$ ),” *Phys. Rev. Lett.* **127**, 217601 (2021).
- [47] T. Schwemmer, H. Hohmann, M. Dürrnagel, J. Potten, J. Beyer, S. Rachel, Y.-M. Wu, S. Raghu, T. Müller, W. Hanke, and R. Thomale, “Sublattice modulated superconductivity in the kagome Hubbard model,” *Phys. Rev. B* **110**, 024501 (2024).
- [48] Y.-M. Wu, R. Thomale, and S. Raghu, “Sublattice interference promotes pair density wave order in kagome metals,” *Phys. Rev. B* **108**, L081117 (2023).
- [49] M. H. Christensen, T. Birol, B. M. Andersen, and R. M. Fernandes, “Theory of the charge density wave in  $\text{AV}_3\text{Sb}_5$  kagome metals,” *Phys. Rev. B* **104**, 214513 (2021).
- [50] M. H. Christensen, T. Birol, B. M. Andersen, and R. M. Fernandes, “Loop currents in  $\text{AV}_3\text{Sb}_5$  kagome metals: Multipolar and toroidal magnetic orders,” *Phys. Rev. B* **106**, 144504 (2022).
- [51] S. Zhou and Z. Wang, “Chern Fermi pocket, topological pair density wave, and charge-4e and charge-6e superconductivity in kagome superconductors,” *Nature Communications* **1**, 7288 (2022).
- [52] H. Li, Y. B. Kim, and H.-Y. Kee, “Intertwined van Hove singularities as a mechanism for loop current order in kagome metals,” *Phys. Rev. Lett.* **132**, 146501 (2024).
- [53] R. Tazai, Y. Yamakawa, S. Onari, and H. Kontani, “Mechanism of exotic density-wave and beyond-Migdal unconventional superconductivity in kagome metal  $\text{AV}_3\text{Sb}_5$  ( $A=\text{K}, \text{Rb}, \text{Cs}$ ),” *Science Advances* **8**, eabl4108 (2022).
- [54] R. Tazai, Y. Yamakawa, and H. Kontani, “Charge-loop current order and  $\mathbb{Z}_3$  nematicity mediated by bond order fluctuations in kagome metals,” *Nature Communications* **14**, 7845 (2023).
- [55] R. Tazai, Y. Yamakawa, and H. Kontani, “Drastic magnetic-field-induced chiral current order and emergent current-bond-field interplay in kagome metals,” *Proceedings of the National Academy of Sciences* **121**, e2303476121 (2024).
- [56] R. Tazai, Y. Yamakawa, T. Morimoto, and H. Kontani, “Quantum-metric-induced giant and reversible nonreciprocal transport phenomena in chiral loop-current phases of kagome metals,” *arXiv preprint arXiv:2408.04233* (2024).
- [57] X. Feng, Z.-T. Sun, B.-C. Lin, and K. Law, “Odd-parity topological superconductivity in kagome metal  $\text{rbv}_3\text{sb}_5$ ,” *arXiv preprint arXiv:2501.10998* (2025).
- [58] S. D. Wilson and B. R. Ortiz, “ $\text{AV}_3\text{Sb}_5$  kagome superconductors,” *Nature Reviews Materials* **9**, 420–432 (2024).
- [59] The switching of the Bragg peaks has since been reproduced in a recent experiment [64].
- [60] In fact, recent avoided level crossing  $\mu\text{SR}$  has suggested there is minimal change in the relaxation rate near  $T_{CDW}$ , with a significant signal near  $T_*$  rather than  $T_{CDW}$  [91].
- [61] C. Guo, M. R. van Delft, M. Gutierrez-Amigo, D. Chen, C. Putzke, G. Wagner, M. H. Fischer, T. Neupert, I. Errea, M. G. Vergniory, S. Wiedmann, C. Felser, and P. J. W. Moll, “Distinct switching of chiral transport in the kagome metals  $\text{KV}_3\text{Sb}_5$  and  $\text{CsV}_3\text{Sb}_5$ ,” *npj Quantum Materials* **9**, 20 (2024).
- [62] J. Lin, private communication.
- [63] Z. Liu, Y. Shi, Q. Jiang, E. W. Rosenberg, J. M. DeStefano, J. Liu, C. Hu, Y. Zhao, Z. Wang, Y. Yao, *et al.*, “Absence of  $E_{2g}$  nematic instability and dominant  $A_{1g}$  response in the kagome metal  $\text{CsV}_3\text{Sb}_5$ ,” *Physical Review X* **14**, 031015 (2024).
- [64] Y. Xing, S. Bae, E. Ritz, F. Yang, T. Birol, A. N. Capa Salinas, B. R. Ortiz, S. D. Wilson, Z. Wang, R. M. Fernandes, *et al.*, “Optical manipulation of the charge density wave state in  $\text{RbV}_3\text{Sb}_5$ ,” *Nature* **631**, 60 (2024).
- [65] C. Guo, G. Wagner, C. Putzke, D. Chen, K. Wang, L. Zhang, M. Gutierrez-Amigo, I. Errea, M. G. Vergniory, C. Felser, *et al.*, “Correlated order at the tipping point in the kagome metal  $\text{CsV}_3\text{Sb}_5$ ,” *Nat. Phys.* **20**, 579 (2024).
- [66] C. Guo, C. Putzke, S. Konyzheva, X. Huang, M. Gutierrez-Amigo, I. Errea, D. Chen, M. G. Vergniory, C. Felser, M. H. Fischer, T. Neupert, and P. J. W. Moll, “Switchable chiral transport in charge-ordered kagome metal  $\text{CsV}_3\text{Sb}_5$ ,” *Nature* **611**, 461 (2022).
- [67] The possibility of a CDW state with domains whose magnetic field or  $C_2$  orientation average to zero is highly unlikely as an explanation for the consistent and reproducible absence of  $C_3$  symmetry breaking observed in low-strain samples. The results of Ref. [65] were demonstrated in flakes of dimension  $\sim 10 - 20$  microns, which would require domains of dimension  $\sim \text{nm}$  for such a cancellation. Setting aside the energetic cost of such nanoscale variations in the charge ordering, there is no evidence for domains of this scale in local probes [24, 27].
- [68] B. Keimer, S. A. Kivelson, M. R. Norman, S. Uchida, and J. Zaanen, “From quantum matter to high-temperature superconductivity in copper oxides,” *Nature* **518**, 179 (2015).
- [69] E. Fradkin, S. A. Kivelson, and J. M. Tranquada, “Colloquium: Theory of intertwined orders in high temperature superconductors,” *Rev. Mod. Phys.* **87**, 457 (2015).
- [70] D. F. Agterberg, J. S. Davis, S. D. Eddins, E. Fradkin, D. J. Van Harlingen, S. A. Kivelson, P. A. Lee, L. Radzihovsky, J. M. Tranquada, and Y. Wang, “The physics of pair-density waves: Cuprate superconductors and beyond,” *Annual Review of Condensed Matter Physics* **11**, 231 (2020).
- [71] G. Wagner, C. Guo, P. J. W. Moll, T. Neupert, and M. H. Fischer, “Phenomenology of bond and flux orders in kagome metals,” *Phys. Rev. B* **108**, 125136 (2023).
- [72] L. Nie, G. Tarjus, and S. A. Kivelson, “Quenched disorder and vestigial nematicity in the pseudogap regime of the cuprates,” *Proceedings of the National Academy of Sciences* **111**, 7980 (2014).
- [73] R. M. Fernandes, P. P. Orth, and J. Schmalian, “Intertwined vestigial order in quantum materials: Nematicity and beyond,” *Annual Review of Condensed Matter Physics* **10**, 133 (2019).
- [74] E. Berg, E. Fradkin, and S. A. Kivelson, “Charge-4e superconductivity from pair-density-wave order in certain

- high-temperature superconductors,” *Nat. Phys.* **5**, 830 (2009).
- [75] P. P. Poduval and M. S. Scheurer, “Vestigial singlet pairing in a fluctuating magnetic triplet superconductor and its implications for graphene superlattices,” *Nature Communications* **15**, 1713 (2024).
- [76] M. Kang, S. Fang, J.-K. Kim, B. R. Ortiz, S. H. Ryu, J. Kim, J. Yoo, G. Sangiovanni, D. Di Sante, B.-G. Park, C. Jozwiak, A. Bostwick, E. Rotenberg, E. Kaxiras, S. D. Wilson, J.-H. Park, and R. Comin, “Twofold van Hove singularity and origin of charge order in topological kagome superconductor  $\text{CsV}_3\text{Sb}_5$ ,” *Nat. Phys.* **18**, 301 (2022).
- [77] Y. Hu, X. Wu, B. R. Ortiz, S. Ju, X. Han, J. Ma, N. C. Plumb, M. Radovic, R. Thomale, S. D. Wilson, A. P. Schnyder, and M. Shi, “Rich nature of van Hove singularities in kagome superconductor  $\text{CsV}_3\text{Sb}_5$ ,” *Nature Communications* **13**, 2220 (2022).
- [78] As an alternative to this microscopic viewpoint, one may consider particle-hole pairing in the  $E_{1u}$  irrep as a postulate of the present work.
- [79] T. Asaba, A. Onishi, Y. Kageyama, T. Kiyosue, K. Ohtsuka, S. Suetsugu, Y. Kohsaka, T. Gaggli, Y. Kasahara, H. Murayama, *et al.*, “Evidence for an odd-parity nematic phase above the charge-density-wave transition in a kagome metal,” *Nat. Phys.* **20**, 40 (2024).
- [80] Certain elastoresistance measurement geometries suffer from contamination – an erroneous response in  $E_{2g}$  can occur due to some mixing with  $A_{1g}$ . Importantly, the *transverse technique* is designed to be free of contamination, and hence we treat it as reliable evidence of a weak  $E_{2g}$  signal.
- [81] E. Day-Roberts, R. M. Fernandes, and T. Birol, “Piezoresistivity as an order parameter for ferroaxial transitions,” *arXiv preprint arXiv:2405.02149* (2024).
- [82] T. Le, Z. Pan, Z. Xu, J. Liu, J. Wang, Z. Lou, X. Yang, Z. Wang, Y. Yao, C. Wu, *et al.*, “Superconducting diode effect and interference patterns in kagome  $\text{CsV}_3\text{Sb}_5$ ,” *Nature* **630**, 64–69 (2024).
- [83] H. D. Scammell, J. I. A. Li, and M. S. Scheurer, “Theory of zero-field superconducting diode effect in twisted trilayer graphene,” *2D Materials* **9**, 025027 (2022).
- [84] J.-X. Lin, P. Siriviboon, H. D. Scammell, S. Liu, D. Rhodes, K. Watanabe, T. Taniguchi, J. Hone, M. S. Scheurer, and J. I. A. Li, “Zero-field superconducting diode effect in small-twist-angle trilayer graphene,” *Nat. Phys.* **18**, 1221 (2022).
- [85] F. Jin, W. Ren, M. Tan, M. Xie, B. Lu, Z. Zhang, J. Ji, and Q. Zhang, “ $\pi$  phase interlayer shift and stacking fault in the kagome superconductor  $\text{csv}_3\text{sb}_5$ ,” *Phys. Rev. Lett.* **132**, 066501 (2024).
- [86] R. Comin, unpublished.
- [87] Here we have only described the Raman process involving a single phonon scattering off a static  $E_{1u}$  condensate; we have neglected processes involving fluctuations of the  $E_{1u}$  order. We leave it for future work to examine the full Raman spectrum induced by  $E_{1u}$  order and fluctuations thereof.
- [88] Here we use point group notation to describe the CDW symmetries; in space group notation,  $A_u$  and  $B_u$  correspond to  $M_1^-$  and  $M_2^-$  respectively.
- [89] S. Ghosh, M. Matty, R. Baumbach, E. D. Bauer, K. A. Modic, A. Shekhter, J. A. Mydosh, E.-A. Kim, and B. J. Ramshaw, “One-component order parameter in  $\text{URu}_2\text{Si}_2$  uncovered by resonant ultrasound spectroscopy and machine learning,” *Science Advances* **6**, eaaz4074 (2020).
- [90] F. Theuss, A. Shragai, G. Grissonnanche, I. M. Hayes, S. R. Saha, Y. S. Eo, A. Suarez, T. Shishidou, N. P. Butch, J. Paglione, and B. J. Ramshaw, “Single-component superconductivity in  $\text{UTe}_2$  at ambient pressure,” *Nat. Phys.* **20**, 1124 (2024).
- [91] P. Bonfà, F. Pratt, D. Valenti, I. J. Onuorah, A. Kataria, P. J. Baker, S. Cottrell, A. Capa Salinas, S. D. Wilson, Z. Guguchia, *et al.*, “Unveiling the nature of electronic transitions in  $\text{RbV}_3\text{Sb}_5$  with avoided level crossing  $\mu\text{SR}$ ,” *arXiv preprint 2411.04848* (2024).
- [92] T. Li, J. Ingham, and H. D. Scammell, “Artificial graphene: Unconventional superconductivity in a honeycomb superlattice,” *Physical Review Research* **2**, 043155 (2020).
- [93] H. D. Scammell, J. Ingham, M. Geier, and T. Li, “Intrinsic first- and higher-order topological superconductivity in a doped topological insulator,” *Phys. Rev. B* **105**, 195149 (2022).
- [94] J. Ingham, T. Li, M. S. Scheurer, and H. D. Scammell, “Quadratic dirac fermions and the competition of ordered states in twisted bilayer graphene,” *arXiv preprint arXiv:2308.00748* (2023).
- [95] D. Guerci, D. Kaplan, J. Ingham, J. Pixley, and A. J. Millis, “Topological superconductivity from repulsive interactions in twisted wse  $_2$ ,” *arXiv preprint arXiv:2408.16075* (2024).

## Appendix A: Effective two-orbital tight binding model

There are three vHS in vicinity of the  $M$ -points, these have orbital character  $d_{zx}, d_{yz}, d_{xy/x^2-y^2}$  [76, 77]. The vHS of predominant  $d_{xy/x^2-y^2}$  character is most strongly reconstructed below  $T_{\text{CDW}}$  [76]. The m-type vHS, of  $d_{yz}$  character, also shows reconstruction, but it is seen to be weaker and moreover the p-type vHS, of  $d_{zx}$  character, is unreconstructed [76]. Based on these observations, our effective two-band model comprises the just  $d_{zx}, d_{yz}$  bands and makes the simplification that  $d_{yz}$  is not reconstructed. The corresponding tight binding model was established in [45]

$$H = \sum_{\mathbf{k}i\alpha} \epsilon_\alpha \psi_{\mathbf{k}i\alpha}^\dagger \psi_{\mathbf{k}i\alpha} - \sum_{\mathbf{k}ij\alpha} t_\alpha \Phi_{ij}(\mathbf{k}) \psi_{\mathbf{k}j\alpha}^\dagger \psi_{\mathbf{k}i\alpha} - t' \sum_{\mathbf{k},ij} \Phi_{ij}(\mathbf{k}) s_{ij} \left( \psi_{\mathbf{k}jxz}^\dagger \psi_{\mathbf{k}iz} - \psi_{\mathbf{k}jyz}^\dagger \psi_{\mathbf{k}ixz} \right). \quad (\text{A1})$$

Here  $\psi_{\mathbf{k}i\alpha}^\dagger$  creates an electron at quasimomentum  $\mathbf{k}$ , sublattice  $i = A, B, C$  and in orbital  $\alpha = xz, yz$ . The lattice hopping factors are  $\Phi_{AB}(\mathbf{k}) = 1 + e^{-2i\mathbf{k}\cdot\mathbf{a}_1}$ ,  $\Phi_{BC}(\mathbf{k}) = 1 + e^{-2i\mathbf{k}\cdot\mathbf{a}_3}$ , and  $\Phi_{AC}(\mathbf{k}) = 1 + e^{-2i\mathbf{k}\cdot\mathbf{a}_2}$  and obey condition

$\Phi_{ij}(\mathbf{k}) = (1 - \delta_{ij}) \Phi_{ji}^*(\mathbf{k})$ . Here we have denoted by  $\mathbf{a}_{1,2} = (\sqrt{3}/2, \pm 1/2)^T$  and  $\mathbf{a}_3 = (0, -1)^T$  the vectors connecting sublattices. The parameters  $\epsilon_\alpha, t_\alpha, t'$  correspond to onsite orbital energy, orbital dependent nearest-neighbour hopping, and an interorbital coupling. Finally,  $s_{ij}$  accounts for the non-trivial spatial symmetry of the interorbital overlap of  $d_{zx}, d_{yz}$ , i.e.  $s_{ij} \in B_{2u}$ . Explicitly, assuming the sublattice sites are labeled according to [45], then  $s_{AC} = s_{CB} = -s_{AB}$  and  $s_{ij} = -s_{ji}$ .

### Appendix B: Meanfield gap equation and $E_{1u}$ excitonic order

We briefly outline the origin of the  $E_{1u}$  excitonic order. The  $E_{1u}$  follows from a direct mean field theory or patch theory treatment (detailed below) and can also be motivated more heuristically as follows. Firstly, a mean field and/or patch theory favours  $E_{2g}$  pairing of the BdG gap function since this provides a full gapping of the Fermi surface and thereby maximises the condensate energy. Second, further account of orbital form-factors introduces an additional  $B_{2u}$  – via reasoning detailed below – and the overall irrep is therefore  $E_{2g} \times B_{2u} = E_{1u}$ . To account for the  $B_{2u}$  orbital form factors, we note that the two vHS exhibit  $m$ - and  $p$ -type sublattice support, and in the case of  $\text{CsV}_3\text{Sb}_5$ , for  $T < T_{\text{CDW}}$  the  $m$ -type vHS are primarily composed of the  $d_{zx}$  orbitals of the vanadium kagome lattice, while the (un-reconstructed)  $p$ -type vHS arises from a band composed of the  $d_{yz}$  orbitals (noting that the  $p$ -type vHS arising from the  $d_{z^2}/d_{x^2-y^2}$  orbitals undergoes significant reconstruction in the CDW phase [76, 77]). Since the  $p$  ( $m$ )-type wavefunctions are inversion even (odd), the product of the band irreps of the TvHS – relevant for excitonic pairing – falls into  $B_{2u}$  of  $D_{6h}$ .

Here we sketch the meanfield gap equation. Decoupling specifically in the excitonic spin-singlet channel, the resulting ‘‘BdG’’ mean-field Hamiltonian is

$$H_{\text{BdG}} = \begin{pmatrix} c_{\mathbf{k}}^\dagger \\ v_{\mathbf{k}}^\dagger \end{pmatrix}^T \begin{pmatrix} \epsilon_{\mathbf{k}}^c & M_{\mathbf{k}} \\ M_{\mathbf{k}}^* & \epsilon_{\mathbf{k}}^v \end{pmatrix} \begin{pmatrix} c_{\mathbf{k}}^\dagger \\ v_{\mathbf{k}}^\dagger \end{pmatrix} = \begin{pmatrix} \tilde{c}_{\mathbf{k}}^\dagger \\ \tilde{v}_{\mathbf{k}}^\dagger \end{pmatrix}^T \begin{pmatrix} \epsilon_{\mathbf{k}}^c & M_{\mathbf{k}} \chi_{\mathbf{k}}^{B_{2u}} \\ M_{\mathbf{k}}^* \chi_{\mathbf{k}}^{B_{2u}} & \epsilon_{\mathbf{k}}^v \end{pmatrix} \begin{pmatrix} \tilde{c}_{\mathbf{k}}^\dagger \\ \tilde{v}_{\mathbf{k}}^\dagger \end{pmatrix}. \quad (\text{B1})$$

In the second equality, we have used that  $(\chi_{\mathbf{k}}^{B_{2u}})^2 = \chi_{\mathbf{k}}^{A_{1g}}$  and further simplified by taking  $\chi^{A_{1g}} \simeq 1$ .

An interaction term, in the excitonic channel, then rescales as

$$V_0 c_{\mathbf{k}_1}^\dagger v_{\mathbf{k}_1} v_{\mathbf{k}_2}^\dagger c_{\mathbf{k}_2} \rightarrow V_0 (\chi_{\mathbf{k}_1}^{B_{2u}} \chi_{\mathbf{k}_2}^{B_{2u}})^2 \tilde{c}_{\mathbf{k}_1}^\dagger \tilde{v}_{\mathbf{k}_1} \tilde{v}_{\mathbf{k}_2}^\dagger \tilde{c}_{\mathbf{k}_2} = \tilde{V}_{0;\mathbf{k}_1,\mathbf{k}_2} \tilde{c}_{\mathbf{k}_1}^\dagger \tilde{v}_{\mathbf{k}_1} \tilde{v}_{\mathbf{k}_2}^\dagger \tilde{c}_{\mathbf{k}_2}. \quad (\text{B2})$$

Following the standard procedure, we obtain the meanfield gap equation in the order parameter  $\tilde{M}_{\mathbf{k}} \equiv M_{\mathbf{k}} \chi_{\mathbf{k}}^{B_{2u}}$ ,

$$\tilde{M}_{\mathbf{k}_1} = \frac{1}{2} \sum_{\mathbf{k}_2} \tilde{V}_{0;\mathbf{k}_1,\mathbf{k}_2} \frac{\tanh\left(\frac{\epsilon_{\mathbf{k}_2}^c}{2T}\right) - \tanh\left(\frac{\epsilon_{\mathbf{k}_2}^v}{2T}\right)}{\epsilon_{\mathbf{k}_2}^c - \epsilon_{\mathbf{k}_2}^v} \tilde{M}_{\mathbf{k}_2}. \quad (\text{B3})$$

Previous work [9] has shown the conditions for the interactions (here denoted  $\tilde{V}_{0;\mathbf{k}_1,\mathbf{k}_2}$ ) to produce  $E_{2g}$  ordering. We therefore do not repeat those lengthy calculations here. Instead, using those results, we infer that a candidate (leading) solution of the gap equation has  $\tilde{M}_{\mathbf{k}} \in E_{2g}$ , and hence  $M_{\mathbf{k}} \in B_{2u} \otimes E_{2g} = E_{1u}$ .

In terms of basis functions,  $B_{2u} = Y_{\mathbf{k}}(3X_{\mathbf{k}}^2 - Y_{\mathbf{k}}^2)$  while  $E_{2g} = \{(X_{\mathbf{k}}^2 - Y_{\mathbf{k}}^2), 2X_{\mathbf{k}}Y_{\mathbf{k}}\}$ . This suggests that the  $E_{1u}$  order for this system is  $\mathcal{E}_{\mathbf{k}}^{E_{1u}} = \{(X_{\mathbf{k}}^2 - Y_{\mathbf{k}}^2), 2X_{\mathbf{k}}Y_{\mathbf{k}}\} Y_{\mathbf{k}}(3X_{\mathbf{k}}^2 - Y_{\mathbf{k}}^2)$ , i.e. excitonic pairing has angular momentum  $|\ell| = 5$ .

### Appendix C: Free energy and coupling to external fields

We consider exciton pairing in a 2D irrep, here explicitly  $E_{1u}$  of  $D_{6h}$ , and further taking the approximate  $\text{SU}(2)_+ \times \text{SU}(2)_-$  spin symmetry to be exact we obtain the allowed terms in the free energy expansion. To begin we define the pairing function  $M_{\mathbf{k}}$  of Eq. (2.2) as

$$M_{\mathbf{k}} = \sum_{\mu=\pm} (X_{\mathbf{k}} + i\mu Y_{\mathbf{k}}) \Delta_{\mu}, \quad \Delta_{\mu} = \sum_{\nu=0}^3 \eta_{\mu\nu} \sigma_{\nu}, \quad (\text{C1})$$

and obtain the action of the symmetries

$$C_{3z} : (\Delta_+, \Delta_-) \longrightarrow (\omega \Delta_+, \omega^* \Delta_-),$$

$$\begin{aligned}
C_{2z} &: (\Delta_+, \Delta_-) \longrightarrow (-\Delta_+, -\Delta_-), \\
C_{2x} &: (\Delta_+, \Delta_-) \longrightarrow (\Delta_-, \Delta_+), \\
\sigma_h &: (\Delta_+, \Delta_-) \longrightarrow (\Delta_+, \Delta_-), \\
\Theta &: (\Delta_+, \Delta_-) \longrightarrow (\Delta_+^\dagger, \Delta_+^\dagger), \\
\text{SU}(2)_+ \times \text{SU}(2)_- &: \Delta_\mu \longrightarrow e^{-i\gamma_+ \cdot \sigma} \Delta_\mu e^{i\gamma_- \cdot \sigma}, \\
\text{U}(1) &: \Delta_\mu \longrightarrow e^{i\theta} \Delta_\mu.
\end{aligned} \tag{C2}$$

Note that the action of the point group symmetries depends on our choice of irrep, which we here take to be  $E_{1u}$ . Armed with these transformations, all allowed terms in the free energy, up to quartic order, are

$$\begin{aligned}
\mathcal{F}_0 &= a \sum_{\mu=\pm} \text{tr} [\Delta_\mu^\dagger \Delta_\mu] + \frac{b_1}{4} \left( \sum_{\mu=\pm} \text{tr} [\Delta_\mu^\dagger \Delta_\mu] \right)^2 \\
&+ \frac{b_2}{2} \sum_{\mu=\pm} \text{tr} [\Delta_\mu^\dagger \Delta_\mu \Delta_\mu^\dagger \Delta_\mu] \\
&+ \frac{b_3}{4} \text{tr} [\Delta_+^\dagger \Delta_+] \text{tr} [\Delta_-^\dagger \Delta_-] + \frac{b_4}{4} \left| \text{tr} [\Delta_+^\dagger \Delta_-] \right|^2 \\
&+ \frac{b_5}{2} \left( \text{tr} [\Delta_+^\dagger \Delta_+ \Delta_-^\dagger \Delta_-] + \text{tr} [\Delta_-^\dagger \Delta_- \Delta_+^\dagger \Delta_+] \right), \\
\mathcal{F}'_0 &= c_1 \sum_{i=x,y} \sum_{\nu=0,x,y,z} \text{Re}(\varphi_0^* \varphi_i d_\nu)^2 + c_2 c_2 \delta_{\nu,0} |d_\nu \varphi|^2
\end{aligned} \tag{C3}$$

Here  $\mathcal{F}'_0$  accounts for explicit breaking of global symmetries: term with coupling constant  $c_1$  accounts for U(1)-breaking, i.e. it contains the background field  $\varphi_0$ , while the term coupling constant  $c_2$  accounts for SO(4)→SO(3) due to spin-exchange interactions.

We consider external probes  $E_i, B_i, \epsilon_{ij}$  and find how they couple to the vestigials (i.e. bilinears in  $\Delta_\mu$ ) in the free energy. We consider only the bilinear in  $\Delta_\mu$  and up to second order in external fields, and only keep non-trivial terms (i.e. the external fields are in a non-trivial irrep). The external fields couple via

$$\begin{aligned}
\delta\mathcal{F}[\mathbf{B}] &= g_1^B B_z \Phi_{A_{2g}}(\bar{d}^* \cdot \bar{d}) - g_2^B \Phi_{A_{1g}} 2\text{Im}(d_0^* \mathbf{d}) \cdot \mathbf{B} + g_3^B B_z \Phi_{A_{2g}} 2\text{Im}(d_0^* \mathbf{d}) \cdot \mathbf{B} + g_4^B (B_x^2 - B_y^2, 2B_x B_y) \cdot \Phi_{E_{2g}}(\bar{d}^* \cdot \bar{d}), \\
\delta\mathcal{F}[\mathbf{E}] &= g_1^E 2\text{Re}(\mathbf{E} \cdot \boldsymbol{\varphi} d_0 \varphi_0^*) + g_2^E (E_x^2 - E_y^2, 2E_x E_y) \cdot \Phi_{E_{2g}}(\bar{d}^* \cdot \bar{d}), \\
\delta\mathcal{F}[\boldsymbol{\epsilon}] &= g^\epsilon \boldsymbol{\epsilon} \cdot \Phi_{E_{2g}}(\bar{d}^* \cdot \bar{d}), \\
\delta\mathcal{F}[\mathbf{B}, \boldsymbol{\epsilon}] &= g^{\epsilon B} \boldsymbol{\epsilon} \cdot \Phi_{E_{2g}} 2\text{Im}(d_0^* \mathbf{d}) \cdot \mathbf{B}, \\
\delta\mathcal{F}[\mathbf{E}, \boldsymbol{\epsilon}] &= g_1^{\epsilon E} \boldsymbol{\epsilon} \cdot (E_x^2 - E_y^2, 2E_x E_y) \Phi_{A_{1g}}(\bar{d}^* \cdot \bar{d}) + g_2^{\epsilon E} (\epsilon_1 \Omega_1 - \epsilon_2 \Omega_2, \epsilon_1 \Omega_2 + \epsilon_2 \Omega_1) \cdot \Phi_{E_{2g}}(\bar{d}^* \cdot \bar{d}), \\
\delta\mathcal{F}[\mathbf{E}, \mathbf{B}] &= \sum_{i=x,y} \sum_{j=x,y,z} g_{ij}^{EB} E_i B_j 2\text{Im}(\varphi_0^* \varphi_i d_j).
\end{aligned}$$

Along the way we introduced  $\{\Omega_1, \Omega_2\} \equiv \{E_x^2 - E_y^2, 2E_x E_y\}$ . Comment: imposing that the conduction and valence bands have a common spin  $g$ -factor, one can show that the axial  $\mathbf{d}^* \times \mathbf{d}$  does not couple to external magnetic field, yet  $\mathbf{d}$  does. The precise values of the coefficients in the free energy can be computed microscopically by integrating out the electrons in a mean-field treatment (see the Supplemental Materials of e.g. Refs. [9, 92–95] for illustration); we leave this calculation to future work.

In the main text Figure 2, the following coefficients were employed:  $g_{ij}^{EB} = 0.5, g_i^B = g_{i'}^E = g^\epsilon = g_{i''}^{\epsilon E} = g^{\epsilon B} = 1$ . (a)  $\epsilon_1 = -\epsilon_2 = \{0, 0.2, 0.4, 0.6\}$   $a = -0.05, b_i = 1, c_1 = 0, c_2 = -0.05$ . (b)  $E_z = B_y = 1$   $\epsilon_1 = -\epsilon_2 = 0.15$   $a = -0.05, b_i = 1, c_1 = 0, c_2 = -0.05$ . (c)  $\epsilon_1 = -\epsilon_2 = 0.15$   $a = -0.05, b_i = 1, c_1 = 0, c_2 = -0.05$ . (d)  $\epsilon_1 = 0.25, \epsilon_2 = 0, a = (T - T_c), T_c = 1, b_i = 1, c_1 = 0, c_2 = -0.05$ .